Rare Metal Materials and Engineering
Volume 54, Issue 11, November 2025
Available online at www.rmme.ac.cn

Science Press

Cite this article as: Wang Mei, Liu Weiming, Peng Buzhuang, et al. Effect of Grain Refinement on Grain Boundary Diffusion Process and Magnetic Properties of Sintered NdFeB Magnets[J]. Rare Metal Materials and Engineering, 2025, 54(11): 2768-2776. DOI: https://doi.org/10.12442/j.issn.1002-185X.20240781.

ARTICLE

Effect of Grain Refinement on Grain Boundary Diffusion Process and Magnetic Properties of Sintered NdFeB Magnets

Wang Mei[1], Liu Weiming[2], Peng Buzhuang[3], Wang Qian[1], Wang Fei[1], Zhang Yumeng[3], Gu Xiaoqian[3], Wang Qi[1], Xiao Guiyong[1], Liu Yan[3], Zhu Xinde[1,4]

[1] Key Laboratory for Liquid-Solid Structural Evolution and Processing of Materials (Ministry of Education), Shandong University, Jinan 250061, China; [2] Yantai Standard and Metrology Inspection and Testing Center, Yantai 264000, China; [3] Yantai Zhenghai Magnetic Material Co., Ltd, Yantai 264006, China; [4] Jianxin Zhao`s Group Co., Ltd, Ningbo 315600, China

Abstract: Three types of NdFeB magnets with the same composition and different grain sizes were prepared, and then the grain boundary diffusion was conducted using metal Tb under the same technical parameters. The effect of grain size on the grain boundary diffusion process and properties of sintered NdFeB magnets was investigated. The diffusion process was assessed using X-ray diffractometer, field emission scanning electron microscope, and electron probe microanalyzer. The magnetic properties of the magnet before and after diffusion were investigated. The results show that the grain refinement of the magnet leads to higher Tb utilization efficiency and results in higher coercivity at different temperatures. It can be attributed to the formation of a deeper and more complete core-shell structure, resulting in better magnetic isolation and higher anisotropy of the $Nd_2Fe_{14}B$ grains. This work may shed light on developing high coercivity with low heavy rare earth elements through grain refinement.

Key words: sintered NdFeB magnets; grain refinement; grain boundary diffusion; coercivity

1 Introduction

Sintered NdFeB magnets are widely used in hard disk drives, new energy vehicles, wind power generation[1], industrial permanent magnet motors, consumer electronic devices, and magnetic medical devices[2], because of their excellent magnetic properties. In recent years, the rapid development of the high-end application market of magnets has promoted innovation in the fabrication techniques of NdFeB magnets, especially the long-term service of magnets at high operating temperatures[3]. Intrinsic coercivity is an important indicator of NdFeB magnets to resist thermal demagnetization, and NdFeB magnets should theoretically have high coercivity to withstand demagnetization at high operating temperatures[4].

Grain boundary diffusion technique is to diffuse heavy rare earth elements into permanent magnets through grain boundary phases under high temperature and vacuum conditions[5–6], which is a major technological innovation in the sintered NdFeB permanent magnet industry in the 21st century. It achieves high coercivity and high magnetic energy product while significantly reducing the use of heavy rare earth elements[7]. For grain boundary diffusion technique, the high-efficiency and low-cost diffusion agents have always been the focus of research. According to the composition of the diffusion agent, it can be divided into three categories. The first type of diffusion agent are mainly pure metals, alloys, and compounds of heavy rare earth elements (Tb and Dy)[8]. During diffusion, Tb/Dy first diffuses along the grain

Received date: December 03, 2024
Foundation item: Key Research and Development Program of Shandong Province (2021CXGC010310); Shandong Province Science and Technology Small and Medium Sized Enterprise Innovation Ability Enhancement Project (2023TSGC0287, 2024TSGC0519); Shandong Provincial Natural Science Foundation (ZR2022ME222); National Natural Science Foundation of China (51702187)
Corresponding author: Zhu Xinde, Ph. D., Associate Professor, Key Laboratory for Liquid-Solid Structural Evolution and Processing of Materials (Ministry of Education), Shandong University, Jinan 250061, P. R. China, E-mail: zhuxinde@sdu. edu. cn; Wang Qian, Ph. D., Key Laboratory for Liquid-Solid Structural Evolution and Processing of Materials (Ministry of Education), Shandong University, Jinan 250061, P. R. China, Email: qian.wang@sdu.edu.cn

boundary phase and then substitutes Nd in the $Nd_2Fe_{14}B$ lattice. As a result, a core-shell type microstructure is obtained as the Tb/Dy diffuses into $Nd_2Fe_{14}B$, forming a $(Nd,Tb/Dy)_2$-$Fe_{14}B$ shell, which magnetically hardens the whole magnet[8]. And consequently, the coercivity of the magnet is greatly improved without or decreasing remanence, while reducing the use of heavy rare earths. The second type of diffusion agent is light rare earth elements, including Nd-Al[9], Pr-Cu[10], and Pr-Al-Cu[11]. This diffusion agent can mainly increase the amount and thickness of non-magnetic grain boundary layers between grains, and better isolate the magnetic coupling between grains, thus increasing the coercivity of the magnet. The third type of diffusion agent is non-rare-earth-based compounds, metals, and alloys[12–15], which work the same way as the second type of diffusion agent.

So far, the most effective diffusion agent for improving coercivity is still the first type. However, the production of large quantities of high coercivity NdFeB magnets containing Dy/Tb faces cost and raw material supply difficulties[8–15]. Therefore, it has become a major issue to reduce the strong dependence of high coercivity NdFeB magnets on heavy rare earths and realize the high efficiency utilization of rare earth resource. Sepehri-Amin et al[16] investigated the grain size dependence of coercivity in NdFeB sintered magnets by finite-element micromagnetic simulations, and attributed an increase in coercivity with a decrease in grain size to the reduction in stray field arising from neighboring grains. Experimental studies[17–19] also have shown that the coercivity of NdFeB magnets increases with the decrease in grain size. However, the coercivity of the sintered magnet is significantly reduced when the grain size is reduced below the critical size (about 3 μm). This is mainly due to the fact that ultrafine powders are easily oxidized in the process of powder metallurgy[20].

By taking advantage of the enhancing effect of grain boundary diffusion and grain refinement on coercivity, it is possible to reduce the amount of heavy rare earths and obtain a higher coercivity at the same time. However, there are few relevant studies on the influence of matrix microstructure changes on the grain boundary diffusion process[21–24], and the mechanism of grain refinement on coercivity has not been studied in detail. In order to understand the effect of grain size on diffusion process and coercivity enhancement, it is necessary to systematically study the microstructure and composition distribution of magnets with different grain sizes after grain boundary diffusion. In this study, non-heavy rare earths matrix magnets with the same composition and different grain sizes were selected as the original magnets, and the changes in microstructure and magnetic properties before and after Tb diffusion were observed through the same diffusion process, so as to find out the internal relationship between grain size and the change in properties after grain boundary diffusion.

2 Experiment

Three types of NdFeB magnets (named S0, S1, and S2) with different grain sizes were fabricated by fully automatic scale casting, hydrogenation powder production, automatic molding, continuous sintering at 1050 °C, and subsequent twice tempering (at 900 and 500 °C for 5 h) in a mixture of N_2, Ar, and H_2 (the base pressure was $<10^{-3}$ Pa), which is called the oxygen-free process technique[25]. Grain size was varied by changing the particle size of jet-milled powders. The obtained NdFeB magnets were selected as the original magnets for Tb diffusion. In order to avoid the influence of rare earth content changes and other process variables on the final analysis results, the three types of samples in this study had the same composition and preparation process parameters except for the process parameters in the jet milling and milling stages. And the subsequent Tb grain boundary diffusion technical parameters were also the same. A self-developed three-dimensional magnetron sputtering apparatus was used to deposit Tb metal film (the mass gain ratio of Tb metal is 0.8%) to the surface of the magnets at room temperature using metallic Tb (purity>99.9%) as a diffusion source, and then grain boundary diffusion was conducted in a high vacuum condition at 900 °C for 10 h, followed by annealing at 500 °C for 2 h. The corresponding magnets after Tb diffusion named as S0D, S1D, and S2D.

The average particle size of the jet-milled powder was measured by a laser particle size analyzer and the corresponding grain size of the sintered magnet (corroded with alcohol and nitric acid) was analyzed by a scanning electron microscope (SEM), as shown in Fig. 1. The main composition design, particle size, and the average grain size of the three types of magnets are shown in Table 1. The magnetic properties of the magnets before and after diffusion were tested at 20, 90, and 140 °C by NIM-10000H hysteresi-graph, separately. The surface phase of the magnets before and after diffusion was studied using DMAX-2500P X-ray diffractometer (XRD) with Cu K-β radiation. JSM-7800F field emission scanning electron microscope (FESEM) was performed for the microstructure observation. The area distribution of the main elements was determined by JXA-8530F Plus electron probe microanalyzer (EPMA).

3 Results

3.1 Grain size and magnetic properties

Fig.2 shows the backscatter electron (BSE) SEM images of S0D, S1D, and S2D and the corresponding grain size distribution, which was calibrated using the diameter of equal area circle of the main grains in Fig. 2 by ImageJ. It can be found that the average grain sizes of S0D, S1D, and S2D magnets, which were fabricated by jet-milled powders with different average particle sizes (as shown in Table 1), are 4.22, 4.06, and 3.47 μm, respectively. Compared to that of sintered NdFeB magnets (S0, S1, S2), as shown in Fig. 1, the main grain size decreases slightly after diffusion, which can be attributed to the formation of Tb-rich shell structure, and the details will be discussed in Section 3.2.

Fig. 3 demonstrates the demagnetization curves of three types of magnets before and after diffusion at 20 °C. The magnetic properties of the magnets are listed in Table 2.

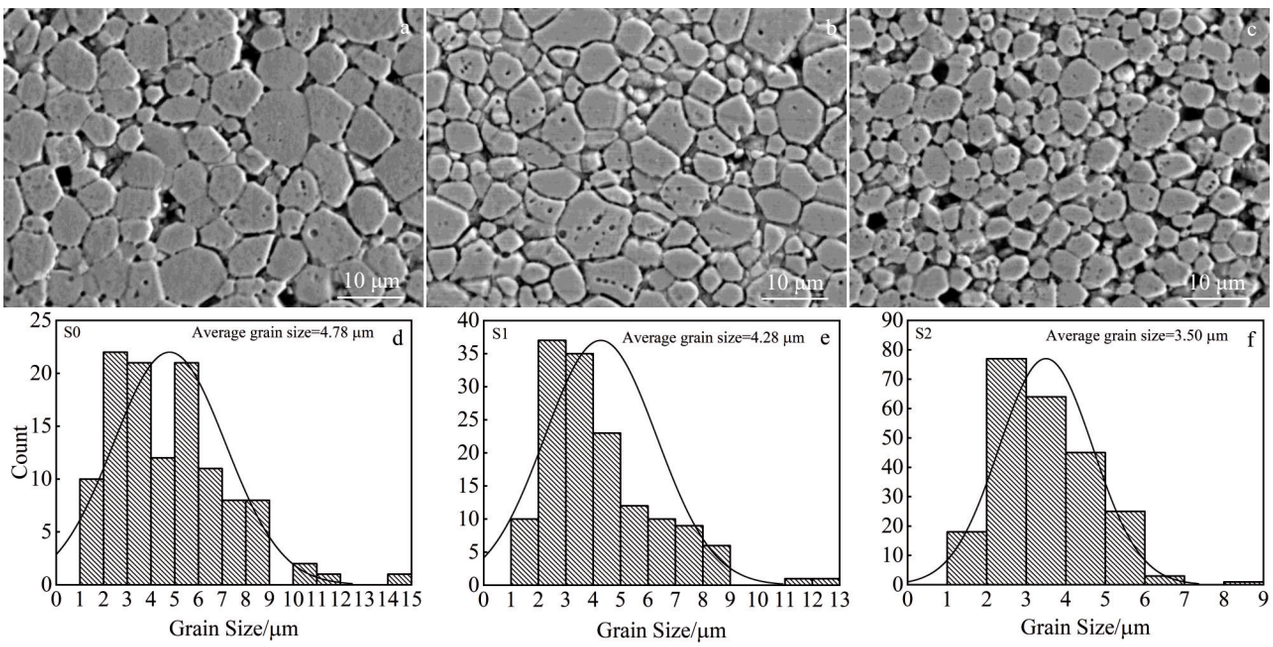

Fig.1 SEM images and corresponding grain size distribution of S0 (a, d), S1 (b, e), and S2 (c, f) magnets

Table 1 Composition, volume mean diameter, and average grain size of original S0, S1, and S2 samples

Sample	Composition/wt%	Volume mean diameter of particle/μm	Average grain size/μm
S0	$Nd_{28.5}Ho_{2.5}Fe_{65.1}B_{1.0}$	5.6	4.78
S1	$Nd_{28.5}Ho_{2.5}Fe_{65.1}B_{1.0}$	4.8	4.28
S2	$Nd_{28.5}Ho_{2.5}Fe_{65.1}B_{1.0}$	3.9	3.50

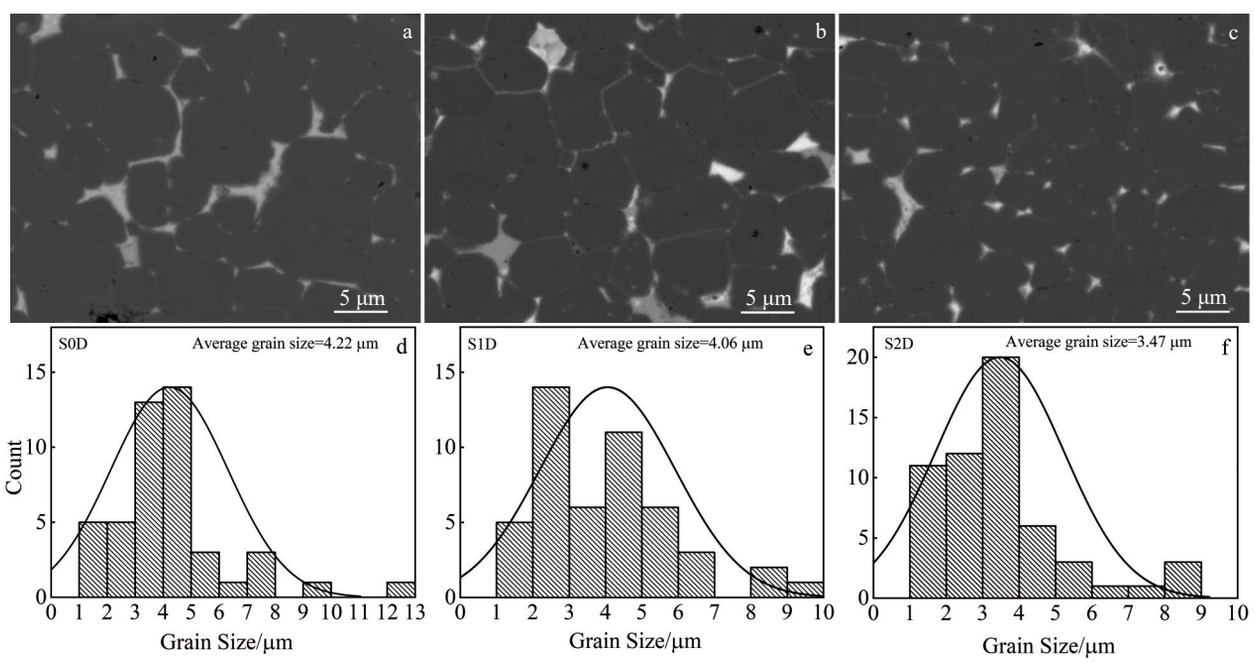

Fig.2 BSE-SEM images and corresponding grain size distribution of S0D (a, d), S1D (b, e), and S2D (c, f) magnets at a diffusion depth of 300 μm

Compared to that of the original magnets, the coercivity of S0D increases from 1.183 T to 2.542 T, S1D increases from 1.254 T to 2.661 T, while S2D increases from 1.278 T to 2.706 T at the same Tb mass gain ratio. It is evident that S2D magnet exhibits the highest coercivity and the highest coercivity increments compared to S0D and S1D magnets, as shown in Fig. 3a, which demonstrates the advantage of the grain refinement in improving coercivity.

The linear *B-H* curve is a very important characteristic that enables the magnets to be stable during operation. Under ideal

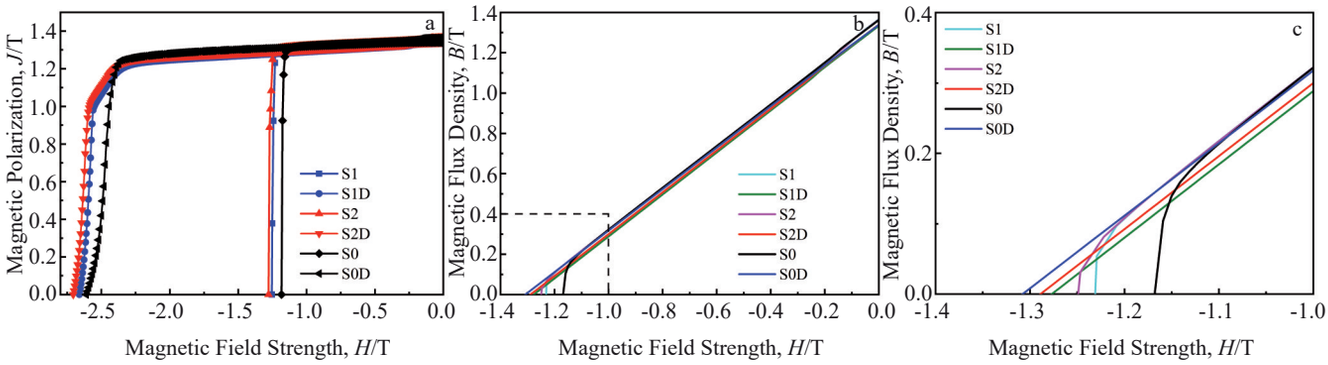

Fig.3 Demagnetization *J-H* (a) and *B-H* (b–c) curves of S0, S1, and S2 magnets before and after Tb diffusion at 20 °C

Table 2 Magnetic properties of magnets before and after Tb diffusion at different temperatures

Sample	Temperature/°C	Magnet remanence, Br/T	Magnetic field strength, *H*/T	Maximum energy product, $(BH)_{max}$/kJ·m^{-3}
S0		1.363	1.183	354.459
S1	20	1.366	1.254	354.220
S2		1.365	1.278	354.538
	20	1.339	2.542	333.046
S0D	90	1.268	1.642	293.406
	140	1.170	1.095	248.432
	20	1.334	2.661	338.061
S1D	90	1.255	1.734	294.918
	140	1.168	1.169	253.446
	20	1.340	2.706	342.996
S2D	90	1.246	1.752	295.634
	140	1.167	1.232	256.232

conditions, it should be a straight line with a slope of 1. Fig.3b depicts magnet flux density (*B*) variations of the S0, S1, and S2 magnets before and after Tb diffusion at 20 °C, reflecting the maximum magnetic energy product $(BH)_{max}$ of the magnets. The *B-H* curves of the S0D, S1D, and S2D magnets (blue line, red line, and green line) show a straight line, while the curves of the original magnets show a knee-like characteristic when the residual magnetism approaches zero. This indicates that the microstructure and density of the magnets are improved after Tb diffusion[8]. As shown in Table 2, the corresponding $(BH)_{max}$ of S0D, S1D, and S2D at 20 °C has values of 333.046, 338.061, and 342.996 kJ·m^{-3}, representing decrease of 6.0%, 4.6%, and 3.3% after diffusion, respectively. It can be seen that magnet grain refinement can weaken the magnetism reduction caused by Tb diffusion.

Fig.4 shows the demagnetization *J-H* and *B-H* curves of the magnets after Tb diffusion at 20, 90, and 140 °C. The magnetic properties of the magnets are listed in Table 2. It can be found that both the coercivity and remanence of the S0D, S1D, and S2D magnets all decrease with increasing temperature, but the S2D magnet possesses the highest coercivity compared to the S0D and S1D magnets at 20, 90, and 140 °C, and the corresponding $(BH)_{max}$ of S2D magnet is also slightly higher than that of the S0D and S1D magnets.

Based on the above results, it can be inferred that the grain refinement of the magnet leads to higher coercivity at different temperatures. The same phenomenon is observed in the Dy diffusion experiment[21].

3.2 Microstructure and elemental distribution

Since the coercivity of NdFeB permanent magnets is extremely sensitive to their microstructure, especially the grain boundary structure and chemistry composition, the phase structure, microstructure, and elemental distribution of the magnets were systematically studied by XRD, FESEM, and EPMA.

XRD diffraction patterns of the six types of samples (S0, S1, S2, S0D, S1D, and S2D) are shown in Fig. 5. As can be seen from Fig. 5a, the main diffraction peaks of six samples are almost identical, mainly (004), (105), and (006), all of which are characteristic peaks of the $Nd_2Fe_{14}B$ phase, which is the magnetic source of the magnet. It is found in both diffused and original magnets that the intensity value of (006) is higher than that of (105), which demonstrates that the *c*-axis orientation of the magnets is substantially preserved after diffusion, showing that all the magnets have good orientation. All characteristic peaks of the original S0 sample are positioned at lower angles than those of original S1 and S2 samples, and all of their characteristic peaks of $Nd_2Fe_{14}B$ matrix phases shift slightly toward a higher angle after Tb

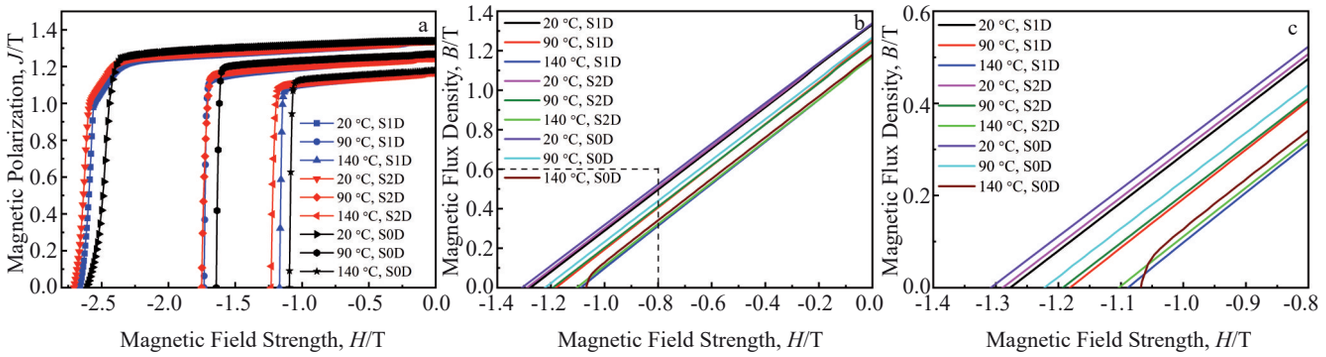

Fig.4 Demagnetization *J*-*H* (a) and *B*-*H* (b–c) curves of magnets after Tb diffusion at 20, 90, and 140 °C

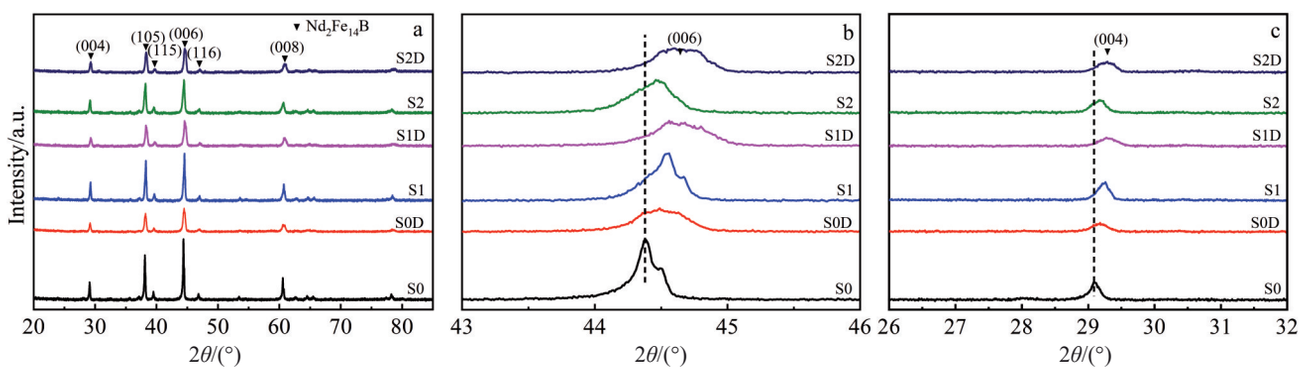

Fig.5 XRD patterns of S0, S1, S2, S0D, S1D, and S2D magnets (a); partially enlarged characteristic peaks of (006) (b) and (004) (c)

diffusion, indicating a reduction in crystal plane spacing (as shown in Fig.5b–5c), which can be attributed to the formation of $(Nd,Tb)_2Fe_{14}B$[26].

BSE images of the magnets before and after Tb diffusion (diffusion depths of 50, 300, and 2750 μm) are shown in Fig. 6. It is known that bright contrast corresponds to phases containing more rare earth elements. The grain boundary of the S1D magnet (Fig.$6b_1$–$6b_2$) is much clearer than that of the S0D and S2D magnets (Fig. $6a_1$–$6a_2$ and Fig. $6c_1$–$6c_2$) at the diffusion depths of 50 and 300 μm, indicating that a thicker Nd-rich phase exists in the S1D magnet.

It can be seen from Fig. $6a_1$, $6b_1$, and $6c_1$ that after Tb diffusion, a bright gray shell forms in the outer region of the $Nd_2Fe_{14}B$ grains in S0D, S1D, and S2D magnets at a depth of 50 μm, and the shell thickness around the main grains of S0D, S1D, and S2D magnets is 0.6–1.8, 0.6–1.2, and 0.3–0.6 μm, respectively. The shell structure of the S2D magnet is not only thinner but also more uniform compared to that of the S0D and S1D magnets. It has been reported that the shell structure is caused by the diffusion of Tb into the $Nd_2Fe_{14}B$ phase and the formation of $(Nd, Tb)_2Fe_{14}B$ shell around main grains[8,17]. Furthermore, at a diffusion depth of 300 μm, a thinner shell than that located at the diffusion depth of 50 μm can be found in the S2D magnet (marked by white arrows in Fig.$6c_2$), while no obvious core-shell structure can be observed in the S1D magnet, which can be attribute to the lower Tb content. This indicates that the fine-grained magnet facilitates the diffusion of Tb into the magnets, resulting in a deeper and clearer shell structure. It demonstrates a higher Tb utilization efficiency in the S2 diffusion process. The core-shell structure cannot be found at the center of all the magnets at the depth of 2750 μm, showing that the Tb content in the center of all three magnets is low.

Fig.7 depicts the EPMA images of the cross-section of S1D and S2D magnets at 0–300 μm depth. The results reveal that the Tb distribution in S2D magnet is more uniform and dispersed from the surface to the depth of 300 μm in comparison to that of the S0D and S1D magnets. There are more element Tb concentrated near the surface of the S0D and S1D magnets than that of the S2D magnet at the same Tb mass gain ratio, indicating that the Tb diffusion in the S2D magnet is relatively more sufficient. The distribution of Nd in the S2D magnet is homogeneous, whereas a large accumulation of element Nd can be observed in the S0D and S1D magnet. In addition, the decrease in Nd concentration near the surface of the magnets can be clearly observed in three types of magnets, as shown by rectangle in red color (Fig.$7a_2$–$7c_2$). The reduction in Nd concentration is attributed to the diffusion of element Nd from the magnet to the coating layer because the Nd-rich liquid phase is present during the diffusion process at 900 °C[27].

To investigate the detailed distribution of elements Tb and Nd in the magnets after diffusion, the element distribution of S0D (Fig.$8a_1$–$8a_3$), S1D (Fig.$8b_1$–$8b_3$), and S2D (Fig.$8c_1$–$8c_3$)

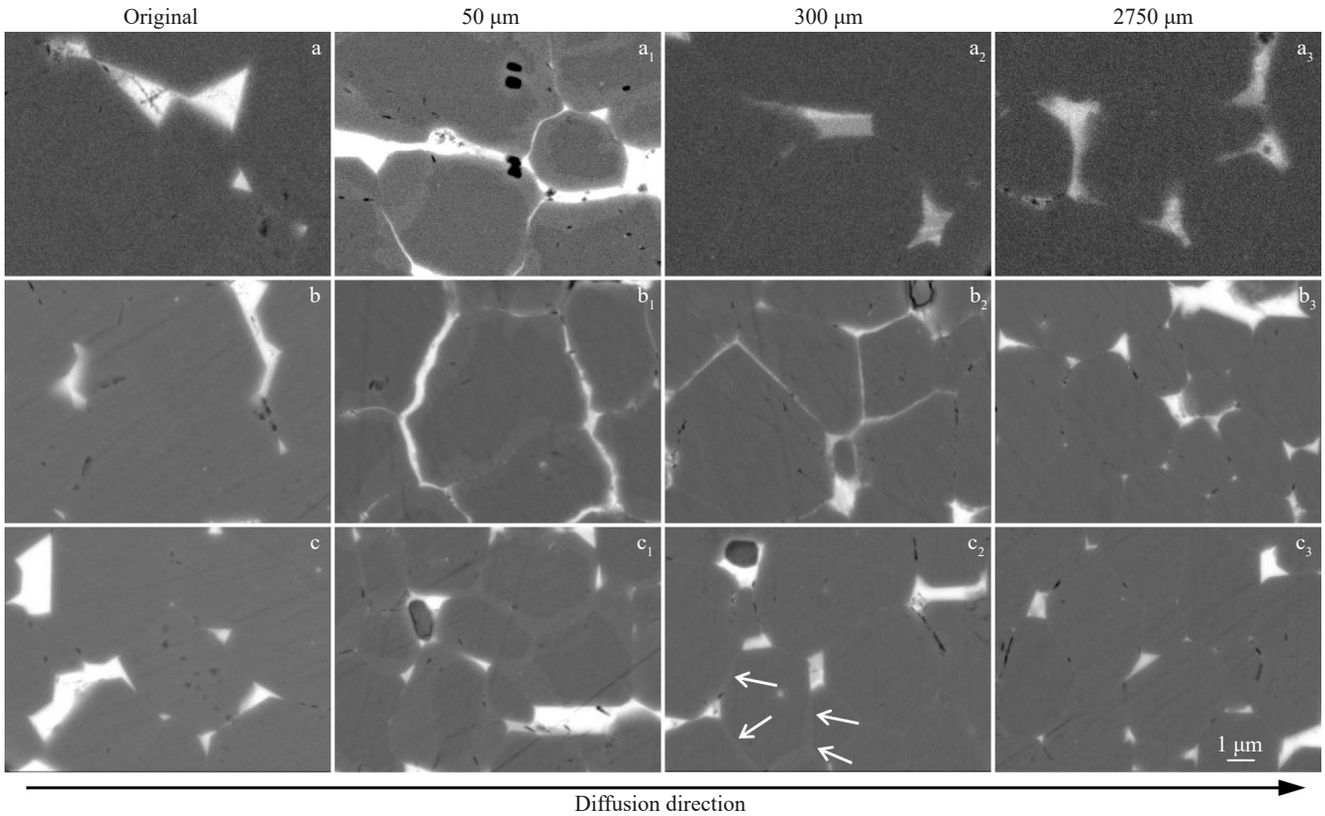

Fig.6 BSE-SEM images of S0 (a), S1 (b), S2 (c), S0D (a_1–a_3), S1D (b_1–b_3), and S2D (c_1–c_3) magnets at different diffusion depths

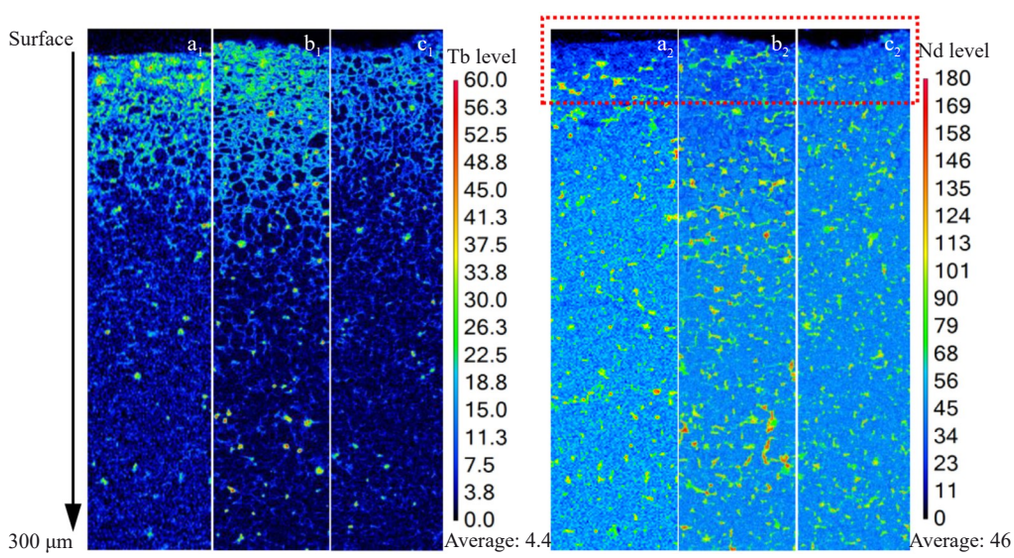

Fig.7 Cross-sectional EPMA images of S0D (a_1–a_2), S1D (b_1–b_2), and S2D (c_1–c_2) magnets at 0–300 μm

magnets at diffusion depths of 100 and 300 μm are analyzed using EPMA. Thicker Nd-rich phase along the grain boundary can be observed in the Nd map of S1D magnet compared to the S0D and S2D magnet. This is consistent with the results in Fig.6.

By comparing the BSE-SEM images in Fig. 2 and the EPMA patterns in Fig.8, it can be seen that the Tb enrichment zone corresponds exactly to the grain boundary position of the magnets, which proves that the diffused element Tb is mainly distributed at the grain boundary of the magnets. As shown in Fig. $6b_1 - 6c_2$, a core-shell structure is obtained as the element Tb diffuses into the $Nd_2Fe_{14}B$ to form a $(Nd, Tb)_2Fe_{14}B$ shell. Here, a well-connected and network-like Tb-rich shell around $Nd_2Fe_{14}B$ grains can be easily found in S0D, S1D, and S2D magnets at diffusion depth of 100 μm. Furthermore, compared with S2D magnet (Fig. $8c_2$),

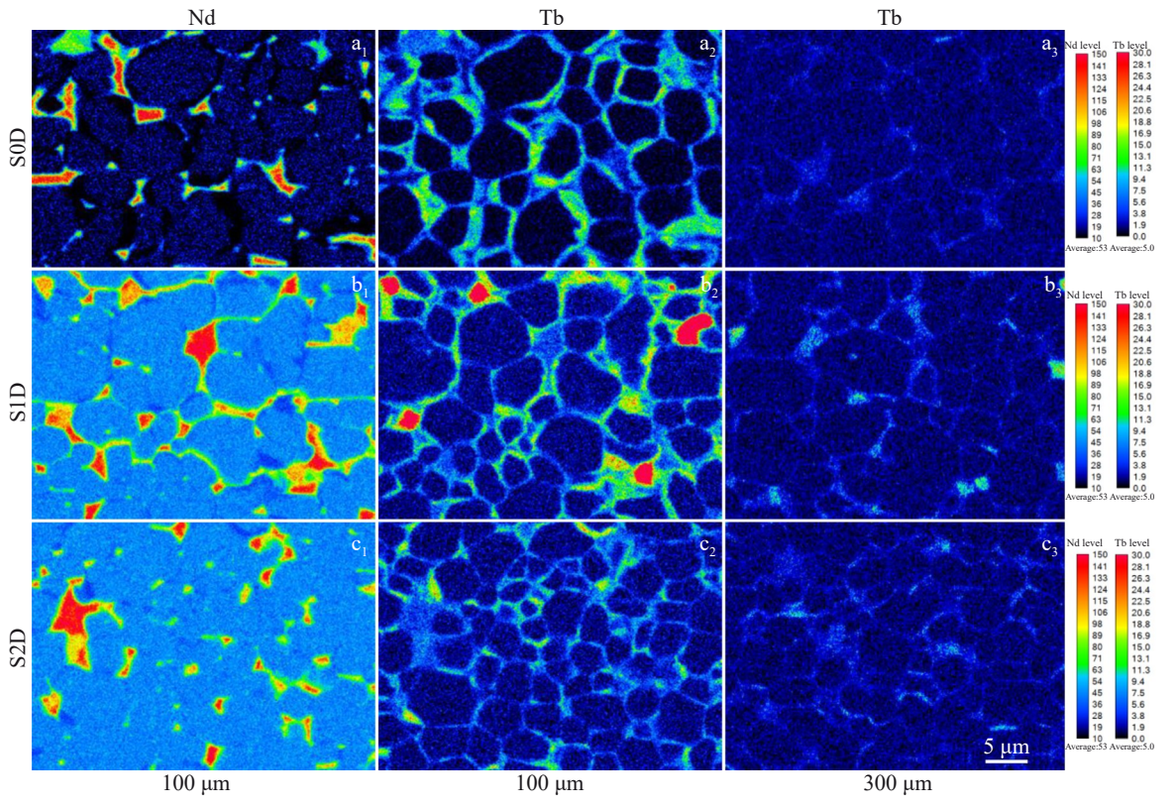

Fig.8 EPMA element mappings of S0D, S1D, and S2D magnets at different diffusion depths of 100 and 300 μm

higher Tb enrichment and higher area fraction of the triple junction phase can be observed in S0D and S1D at the same Tb mass gain ratio. However, at diffusion depth of 300 μm, the well-connected and network-like Tb enrichment still can be observed in S2D magnet (Fig. 8c_3), while S0D magnet shows the least continuous Tb enrichment along the grain boundary (Fig. 8a_3). It can be inferred that the Tb distribution in S2D magnet is fairly homogeneous and continuous, confirming that the Tb diffusion in S2D magnet is more sufficient than that in S0D and S1D magnets. This is consistent with the results in Fig.6.

4 Discussion

Fig. 9 displays the schematic diagram of grain boundary diffusion for coarse-grained (Fig.9a) and fine-grained (Fig.9b) magnets. The number of magnet grain boundaries is increased due to grain refinement, which increases the diffusion channels of element Tb. In other words, grain refinement will increase diffusion depth along the grain boundary in the magnet, so the diffusion efficiency of Tb in fine-grained magnet is better than that in coarse-grained magnets. This is consistent with the results observed in Fig. 6 and Fig. 8. A similar situation has been reported in a previous report[28]. In addition, due to the refinement of the main phase grains, more grain boundary layers are formed, fine-grained magnets have higher defect densities and greater grain boundary distortion energies, which provide a greater driving force for element diffusion[6]. Since the atoms in the grain boundary layer are in a high energy state, it is extremely easy to undergo atomic transitions and form vacancies after thermal activation, promoting the diffusion of heavy rare earth elements along the interface of the grain boundary layer. It is equivalent to the auxiliary path of the grain boundary layer as an element diffusion channel, which expands the diffusion path of the element. Moreover, these auxiliary paths are continuous and almost defect-free[28–29]. Therefore, the diffusion of heavy rare earths in fine-grained magnets is more uniform and more sufficient than that in coarse-grained magnets.

The diffusion of heavy rare earth elements in the magnet is not only along the grain boundaries to the interior of the magnet, but also from the grain boundaries to the interior of the main phase grains. The higher the concentration of heavy rare earth elements at the grain boundaries, the more heavy rare earth elements diffuse into the main phase grains through the grain boundaries, resulting in the formation of a thicker shell structure on the periphery of the main phase grains. In coarse-grained magnets, the concentration of Tb near the surface (at diffusion depths of 50 and 100 μm) is higher, the diffusion of heavy rare earth elements to the main phase grains is stronger, and the shell structure of $(Nd,Tb)_2Fe_{14}B$ is thicker (as shown in Fig. 6 and Fig. 8). However, the concentration of Tb close to the sample center is higher in fine-grained magnets and a clearer shell structure can be observed at a diffusion depth of 300 μm (as shown in Fig. 6 and Fig.8).

After grain boundary diffusion, the coercivity of magnets

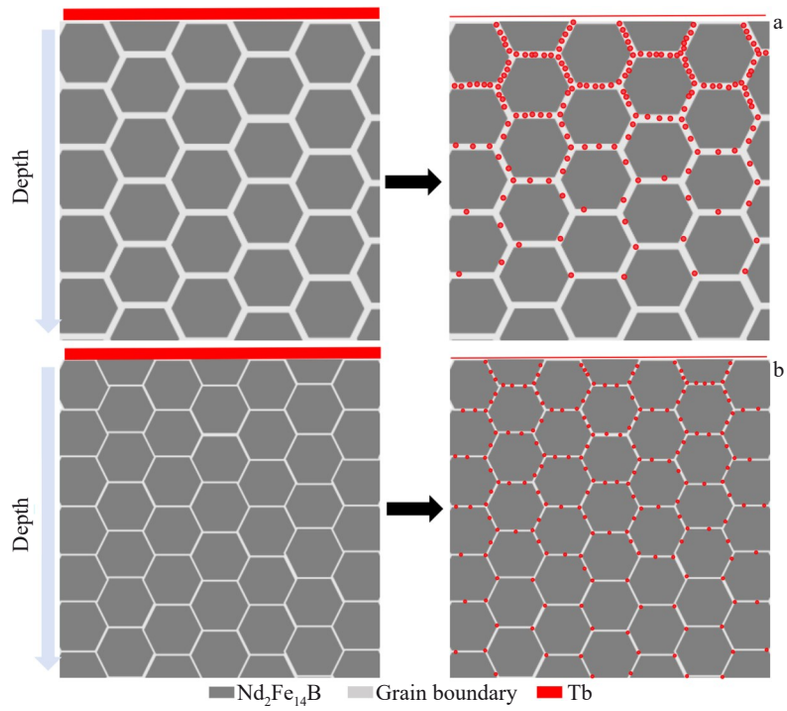

Fig.9 Schematic diagrams of grains boundary diffusion for coarse-grained magnet (a) and fine-grained magnet (b)

increases due to two main factors. Firstly, the formation of a core-shell structure enhances the magnetocrystalline anisotropy field of the defect layer on the grain surface. Nevertheless, if the shell structure is too thick, it will cause the waste of heavy rare earth elements in the diffusion process, and will also lead to the decrease in Br. Secondly, the increased grain boundary phase results in a better magnetic isolation effect among grains. Therefore, the difference in the concentration distribution of heavy rare earths in magnets with different grain sizes results in differences in coercivity.

The S2D magnet exhibits a deeper and more complete core-shell structure when compared to the S0D and S1D magnets, resulting in a better magnetic isolation and higher-anisotropy of the $Nd_2Fe_{14}B$ grains with the formation of the Tb-rich shell. However, the S1D magnet shows thicker Nd-rich phase along grain boundaries, which can better wrap the $Nd_2Fe_{14}B$ grains and strengthen the demagnetization coupling effect. As discussed in Section 3.1, the S2D magnet possesses a higher coercivity than the S1D magnet. It can be considered that the shell structure formed by the Tb substitution is the main factor of the coercivity enhancement in the grain boundary diffusion process. The deeper diffusion depth of heavy rare earth elements makes the distribution of Tb in the magnet more uniform, with higher concentration in the deep shell structure, which is the reason for the greater increase in coercivity after the diffusion of magnets with finer grains. In addition, as shown in Table 2, most of the magnetic properties of S2D magnets are better than those of S0D and S1D magnets, which can be attributed to the more homogeneous and deeper distribution of Tb, resulting in less antiferromagnetic coupling between Tb and Fe.

5 Conclusions

1) For the NdFeB magnets with different grain sizes and the same composition, the formation of a deeper and more complete core-shell structure in the fine-grained (S2D) magnets demonstrates that the grain refinement allows more Tb to diffuse deep into the magnet, resulting in better magnetic isolation and higher anisotropy degree of the $Nd_2Fe_{14}B$ grains. The coarse-grained (S1D) magnet shows a thicker Nd-rich phase than the fine-grained magnet, which can better wrap the $(Nd)_2Fe_{14}B$ grains and strengthen the demagnetization coupling effect. Fine-grained magnet displays higher coercivity at different temperatures compared with the coarse-grained magnet.

2) It can be considered that the core-shell structure formed by the Tb substitution is the main factor of the coercivity enhancement in the grain boundary diffusion process. Thus, the grain size of the original magnets can affect the grain boundary diffusion process and determine the microstructure and coercivity.

References

1 Li L, Post B, Kunc V *et al*. *Scr Mater*[J], 2017, 135: 100
2 Brown D N, Wu Z, He F *et al*. *J Phys: Condens Matter*[J], 2014, 26: 064202
3 Zuo Siyuan, Li Yajing, Zheng Liyun *et al*. *J Chin Soc Rare Earths*[J], 2024, 42(1): 1 (in Chinese)
4 Li J N, Sepehri-Amin H, Sasaki T *et al*. *Adv Mater*[J], 2021, 22(1): 386
5 Nakamura H, Hirota K, Shimao M. *IEEE Trans Magn*[J], 2005,

41: 3844
6 Liu Z W, He J Y, Zeng C C *et al*. *J Magn Mater Devices*[J], 2023, 54(4): 97
7 Zhou T J, Chen J, Wang Q R *et al*. *Journal of Alloys and Compounds*[J], 2023, 937: 168368
8 Zhu X D, Wang M, Yu Y J *et al*. *Crystals*[J], 2023, 13: 1516
9 Sepehri-Amin H, Prabhu D, Hayashi M *et al*. *Scr Mater*[J], 2013, 68: 167
10 Lu K C, Bao X Q, Tang M H *et al*. *J Magn Magn Mater*[J], 2017, 441: 517
11 Zeng H X, Liu Z W, Zhang J S *et al*. *J Mater Sci Technol*[J], 2020, 36: 50
12 Zhou Q, Liu Z W, Zhong X C *et al*. *Mater Des*[J], 2015, 86: 114
13 Chen W, Huang Y L, Luo J M *et al*. *J Magn Magn Mater*[J], 2019, 476: 134
14 Wang E H, Xiao C H, He J Y *et al*. *Appl Surf Sci*[J], 2021, 565: 150545
15 He J Y, Liao X F, Lan X X *et al*. *J Alloys Compd*[J], 2021, 870: 159229
16 Sepehri-Amin H, Ohkubo T, Gruber M *et al*. *Scr Mater*[J], 2014, 89: 29
17 Uestuener K, Katter M, Rodewald W. *IEEE Trans Magn*[J], 2006, 42(10): 2897
18 Chen L, Cao X J, Guo S *et al*. *IEEE Trans Magn*[J], 2015, 51(11): 2101403
19 Guo S, Yang X, Fan X *et al*. *Materials*[J], 2022, 15: 4987
20 Li W F, Ohkubo T, Hono K *et al*. *J Magn Magn Mater*[J], 2009, 321:1100
21 Cheng Xinghua, Li Jian, Liu Tao *et al*. *J Chin Soc Rare Earths*[J], 2020, 38(6): 752 (in Chinese)
22 Zhao Changyu, Liu Ying, Zhao Wei *et al*. *Rare Metal Materials and Engineering*[J], 2023, 52(1): 74
23 Chen Kan, Zhao Hongliang, Fan Fengchun. *Rare Metal Materials and Engineering*[J], 2024, 53(3): 841 (in Chinese)
24 He J Y, Yu Z G, Cao J L *et al*. *J Mater Chem C*[J], 2022, 10: 2080
25 Xie Hongzu. *Theory and Practice of NdFeB Oxygen Free Process Technology*[M]. Beijing: Metallurgical Industry Press, 2018: 21 (in Chinese)
26 Zhou T J, Liu R H, Qu P P *et al*. *J Mater Res Technol*[J], 2022, 20: 1391
27 Liu R H, Qu P P, Zhou T J *et al*. *J Magn Magn Mater*[J], 2021, 536: 168091
28 Luo Shuguang. *Effect of Grain Size on Grain Boundary Diffusion Process and Properties of Sintered NdFeB*[D]. Ganzhou: Jiangxi University of Science and Technology, 2022 (in Chinese)
29 Ramesh R, Thomas G, Ma B M. *J Appl Phys*[J], 1988, 64(11): 6416

晶粒细化对烧结钕铁硼晶界扩散过程及磁性能的影响

王　美[1]，刘伟明[2]，彭步庄[3]，王　倩[1]，王　飞[1]，张玉孟[3]，顾晓倩[3]，王　琦[1]，
肖桂勇[1]，刘　艳[3]，朱新德[1,4]

(1. 山东大学 材料液固结构演化与加工教育部重点实验室，山东 济南 250061)

(2. 烟台市标准计量检验检测中心，山东 烟台 264000)

(3. 烟台正海磁性材料有限公司，山东 烟台 264006)

(4. 建新赵氏集团有限公司，浙江 宁波 315600)

摘　要：制备了3种成分相同、晶粒尺寸不同的钕铁硼磁体，并在相同的技术参数下使用金属Tb进行了晶界扩散。使用X射线衍射、场发射扫描电子显微镜和电子探针显微分析仪评估扩散过程并对磁体扩散前后的磁性能进行了表征，研究了晶粒尺寸对烧结NdFeB磁体晶界扩散过程和性能的影响。结果表明，磁体的晶粒细化可以提高Tb扩散效率，并使磁体在不同温度下具有更高的矫顽力。这主要是由于在晶界扩散过程中磁体内部形成了更深、更完整的核壳结构，从而使$Nd_2Fe_{14}B$晶粒具有更好的磁隔离和各向异性。研究表明在低含量重稀土元素的情况下，细化晶粒可以提高磁体矫顽力。

关键词：烧结NdFeB；晶粒细化；晶界扩散；矫顽力

作者简介：王　美，女，1983年生，博士，副教授，山东大学材料液固结构演化与加工教育部重点实验室，山东 济南 250061，E-mail：wangmei@sdu.edu.cn